DOI 10.1007/s11141-021-10130-7
Radiophysics and Quantum Electronics, Vol. 64, No. 4, September, 2021
(Russian Original Vol. 64, No. 4, April, 2021)

FORMATION OF INTENSE ATTOSECOND PULSES IN THE SEQUENCE OF A RESONANT ABSORBER AND ACTIVE MEDIUM OF A PLASMA-BASED X-RAY LASER MODULATED BY AN OPTICAL FIELD

I. R. Khairulin,[1] **V. A. Antonov,**[1*] **and O. A. Kocharovskaya** [2]

UDC 535.3

We study the possibility of transforming quasi-monochromatic seeding X-ray radiation into an attosecond pulse train in the system composed of a resonant absorber (the plasma of hydrogen-like ions) and an active medium of a plasma-based X-ray laser (the plasma of identical ions in the excited state), which are modulated by the same optical field. In this case, the formation of pulses occurs in a modulated absorber, while the active medium is used for their subsequent amplification. It is shown that this approach significantly increases the energy of the pulses and improves their shape in comparison with the pulse formation directly in the modulated active medium of an X-ray laser. The obtained analytical solution shows that the pulse formation in the modulated absorber is due to the existence of a multifrequency structure of the resonant radiation, which propagates in the medium without absorption. It is shown, both analytically and numerically, that the spectral–temporal characteristics of the pulses are insensitive to changes in the optical thickness of each medium (absorbing and amplifying) over a wide range. The possibility of forming X-ray pulses with a wavelength of the order of 3.4 nm, having a duration of less than 200 as and a peak intensity exceeding $10^{13}\,\mathrm{W/cm^2}$*, in the plasma of hydrogen-like* C^{5+} *ions is shown.*

1. INTRODUCTION

Pulse radiation of the X-ray and vacuum ultraviolet (VUV) wavelength ranges is a unique tool for studying the structure and dynamics of different media on femtosecond [1–6] and attosecond [6–10] time scales. At present, these studies are conducted using the radiation of free electron lasers [11, 12] or sources based on the generation of high-order harmonics of the visible or infrared laser field [7, 9, 12]. Herein, free electron lasers are distinguished by a peak intensity of X-ray radiation (up to $10^{18}\,\mathrm{W/cm^2}$), although, as a rule, they are characterized by a low spatial and temporal coherence. At the same time, the generation of high-order harmonics makes it possible to achieve high coherence and form pulses of VUV and X-ray radiation with a record-short duration (less than 50 as), but low energy in the X-ray range.

Plasma-based X-ray lasers [13–16] represent a different class of VUV and soft X-ray radiation sources. As a rule, these lasers provide a better coherence in comparison with free electron lasers and a higher pulse energy in comparison with sources based on the high-order harmonic generation. The main restriction preventing the use of plasma-based X-ray lasers for sounding the dynamics of rapid processes is the significant (usually picosecond) duration of the radiated pulses. In recent years, the possibility of reducing the duration

* antonov@appl.sci-nnov.ru

[1] Institute of Applied Physics, Russian Academy of Sciences, Nizhny Novgorod, Russia; [2] Department of Physics and Astronomy and Institute for Quantum Studies and Engineering, Texas A&M University, College Station, USA. Translated from Izvestiya Vysshikh Uchebnykh Zavedenii, Radiofizika, Vol. 64, No. 4, pp. 300–319, April 2021. Russian DOI: 10.52452/00213462_2021_64_04_300 Original article submitted April 12, 2021; accepted April 29, 2021.

of plasma-based X-ray laser radiation to tens (in theory) and hundreds (in experiment) of femtoseconds by increasing the number density of free electrons [17, 18] and amplifying the frequency-modulated seeding radiation (one of the harmonics of the high-order optical field) with subsequent compensation for frequency modulation has been shown [19, 20].

Shorter pulses can be generated and amplified on the basis of a method proposed by the authors of this paper. The method includes expanding the amplification spectrum of a plasma-based X-ray laser due to the modulation of its active medium by an intense optical field propagating together with the resonant seeding radiation [21–25]. The role of the optical field in this case consists of rapid (on the optical period scale) modulation of the position of the energy levels of resonant ions in time and space due to the Stark effect. The position of the energy levels of the ions changes following the optical field oscillations, which leads to harmonic (with an optical frequency) modulation of the frequency of the inverted transition and enrichment of the amplification spectrum of the active medium with combination frequencies that are separated from the time-average transition frequency by a multiple of twice the optical frequency. As a result, it becomes possible to amplify the sequence of attosecond pulses formed during the generation of high-order harmonics of the modulating field [22, 25], as well as the possibility of forming a sequence of subfemtosecond pulses directly in the modulated active medium of a plasma-based X-ray laser during the amplification of quasi-monochromatic seeding radiation (e. g., a single harmonic of a high-order optical field) [21, 23, 24]. However, the capabilities of the latter method are limited by controversial requirements to the medium parameters necessary for the formation and amplification of pulses. The formation of pulses requires effective generation of combination frequencies by quasi-monochromatic seeding radiation, which implies a weak plasma dispersion at the frequency of the modulating field, i. e., a greater coherence length compared to the amplification length [21, 23, 24], while effective amplification requires the fulfillment of the opposite condition [22, 25].

It is shown in the paper that this contradiction can be resolved and, accordingly, the characteristics of the generated attosecond pulses can be significantly improved if an additional plasma layer of resonantly absorbing ions similar to those of the active medium is placed in front of the active medium of the X-ray laser. The additional layer is modulated by the same optical field as the active medium. In this case, the expansion of the spectrum of the quasi-monochromatic seeding radiation and the formation of attosecond pulses occur in a modulated resonant absorber [26], which enables one to obtain pulses with a shorter duration and a better shape (greater contrast and duty factor) than in the amplifying medium [24]. In this case, the modulated active medium acts as an amplifier of a pre-formed pulse sequence [22], which makes it possible to significantly increase its optical thickness and achieve a higher intensity of the amplified signal (by means of a more intense amplified spontaneous radiation) compared to the formation of pulses directly in the active medium. In addition, the shape and duration of the pulses are insensitive to changes in the thickness of each medium over a wide range.

The paper is organized as follows: the main approximations and basic equations are formulated in Sec. 2. Section 3 contains the derivation of an analytical solution for X-ray radiation transformed into a sequence of two media, passive (resonantly absorbing) and active (amplifying), modulated by the same intense optical field. In the part concerning the resonant absorber, this solution is considerably more general than the analytical solution published in [26] and makes it possible to draw new conclusions about the conditions for the formation of pulses in a passive medium and their characteristics. In addition, the optimal conditions for the formation of pulses in the sequence of passive and active media corresponding to the shortest duration and the best shape of the pulses are determined on the basis of the analytical solution. Section 4 is devoted to the analysis of a more general nonlinear system of equations. This section presents the results of numerical simulations applied to a set of passive and active media based on hydrogen-like C^{5+} ions. Numerical solutions are compared with analytical ones, as well as with the results of simulations for the formation of pulses directly in the active medium of a plasma-based X-ray laser [24]. The effects that were not taken into account in the analytical solution are studied. The main results of the work are formulated in the Conclusions.

2. THEORETICAL MODEL

Consider a sequence of two media, passive (resonantly absorbing) and active (amplifying), each of which is the plasma of hydrogen-like C^{5+} ions and has the shape of a narrow cylinder stretched along the x axis. An active medium with population inversion at the transition $n_{\rm pr} = 1 \leftrightarrow n_{\rm pr} = 2$ (where $n_{\rm pr}$ is the principal quantum number) of C^{5+} ions can be created by a high-intensity (with an intensity of about $10^{19}\,{\rm W/cm^2}$) femtosecond optical pump pulse [27]. Population inversion is achieved as a result of complete optical ionization of the medium (separation of all electrons from carbon atoms) and subsequent recombination of electrons into highly excited states of C^{5+} ions, as well as radiative and non-radiative transitions, as a result of which the ions are in states with $n_{\rm pr} = 2$. As is shown in [27], the active medium, along with the carbon ions, must contain light ions, e. g., H^+ ions to increase the population inversion; at the same time, characteristic values of the number density of resonant C^{5+} ions and free electrons in the active medium are $N_{\rm ion}^{\rm (act)} = 10^{19}\,{\rm cm^{-3}}$ and $N_{\rm e}^{\rm (act)} = 1.5 \cdot 10^{20}\,{\rm cm^{-3}}$, respectively [22, 27]. A passive medium can be obtained in a similar way: after the optical ionization of carbon by an intense laser field, most of the C^{5+} ions will be in the ground state with $n_{\rm pr} = 1$ over a certain period of time. The number density of resonant carbon ions in a passive medium can vary over a wide range. Next, we assume the number density to be equal to $N_{\rm ion}^{\rm (pas)} = 10^{17}\,{\rm cm^{-3}}$, similar to [21, 24]. Herein, we consider that the resonantly absorbing plasma is obtained as a result of the ionization of pure carbon and the number density of free electrons in the plasma is $N_{\rm e}^{\rm (pas)} = 5 \cdot 10^{17}\,{\rm cm^{-3}}$. Thus, in the case under consideration, the passive medium is significantly less dense in comparison with the active one. Nevertheless, the main conclusions of the paper are also valid for higher density numbers of ions and electrons in a passive medium with a proportional decrease in its thickness.

After the creation of the passive and active media a certain time has passed, which is sufficient for C^{5+} ions to accumulate in the ground state with $n_{\rm pr} = 1$ in the passive medium and in the excited states with $n_{\rm pr} = 2$ in the active medium. The sequence of these media is irradiated by the combination of a modulating optical field with an intensity of about $10^{16}\,{\rm W/cm^2}$ (the optical field almost does not ionize C^{5+} ions) and quasi-monochromatic resonant seeding X-ray radiation with a wavelength of about 3.4 nm. The pulses of the modulating field and resonant radiation propagate along the x axis in each medium together (they overlap in time and space) and have the same linear polarization oriented along the z axis (see [24]).

The modulating optical field has a picosecond duration and can be approximated by a monochromatic wave on the scale of a femtosecond pulse of resonant radiation

$$\mathcal{E}_{\rm L}(x,t) = \mathbf{z}_0 E_{\rm L} \cos[\Omega(t - n_{\rm pl}x/c)], \tag{1}$$

where $\mathbf{z}_0$ is a unit vector along the z axis, Ω and $E_{\rm L}$ are the frequency and amplitude of the optical field, respectively, c is the speed of light in empty space, $n_{\rm pl} = \sqrt{1 - 4\pi N_{\rm e} e^2/(m_{\rm e}\Omega^2)}$ is the refractive index of the plasma at the frequency of the optical field (different for passive and active media), $N_{\rm e}$ is the number density of free electrons (in a particular medium), and $m_{\rm e}$ and e are their mass and charge, respectively. During propagation in the medium, the modulating field is affected by the plasma dispersion. However, the modulating field retains its spatial structure due to the presence of a plasma channel formed during the pre-ionization of the plasma (see, e. g., [17]). A similar effect can be achieved due to a microcapillary [28]. At the same time, the absorption and reflection of the modulating field in the plasma are insignificant due to the fact that the frequency of the field is many times lower than the frequencies of quantum transitions from populated states of ions and, along with it, significantly (at least by one or two orders of magnitude) exceeds the frequencies of plasma oscillations in the active and passive media.

Simultaneously with the modulating field (1), the sequence of passive and active media is irradiated with quasi-monochromatic seeding radiation of the X-ray spectral range. At the front boundary of the passive medium, at $x = 0$, the X-ray radiation has the form

$$\mathbf{E}(x = 0, t) = \frac{1}{2}\mathbf{z}_0 \tilde{E}_{\rm inc}(t) \exp(-i\omega_{\rm inc} t) + c.\,c., \tag{2}$$

where $\tilde{E}_{\rm inc}(t)$ is the slowly varying amplitude of the seeding radiation, $\omega_{\rm inc}$ is its carrier frequency, and c. c. denotes complex conjugation. During propagation in a resonant absorber, the X-ray spectrum is enriched with the combination frequencies $\omega_{2k} = \omega_{\rm inc} + 2k\Omega$, where k is an integer [26], and the X-ray radiation is already multi-frequency at the front boundary of the active medium.

The equations describing the propagation of resonant radiation in a plasma active medium with population inversion at the transition $n_{\rm pr} = 1 \leftrightarrow n_{\rm pr} = 2$ of hydrogen-like ions modulated by an intense optical field are given in [22–25]. The propagation of radiation in a passive medium is described by the same equations with different initial conditions for the quantum state of the medium [26]. Further, we reproduce the equations from [25] in a reduced form (their analytical solution is fundamentally new).

The excited energy levels of ions are Stark-split under the action of a modulating field. In particular, the energy level with $n_{\rm pr} = 2$ is split into three sublevels. Two of them are eigenstate hydrogen-like ions in the parabolic coordinate system $|2\rangle = (|2s\rangle + |2p, m_{\rm mag} = 0\rangle)/\sqrt{2}$ and $|3\rangle = (|2s\rangle - |2p, m_{\rm mag} = 0\rangle)/\sqrt{2}$, where $m_{\rm mag}$ characterizes the projection of the orbital momentum of ions on the z axis. As a result of the linear Stark effect, the energies of these states follow the local value of the electric field (1) in time and space, and the quadratic Stark effect leads to a constant shift of the energies:

$$\hbar\omega_2(t,x) = -\frac{m_{\rm e}e^4Z^2}{8\hbar^2}\left\{1 + \frac{21}{4}F_0^2 + 3F_0\cos\left[\Omega\left(t - \frac{n_{\rm pl}}{c}x\right)\right]\right\},$$
$$\hbar\omega_3(t,x) = -\frac{m_{\rm e}e^4Z^2}{8\hbar^2}\left\{1 + \frac{21}{4}F_0^2 - 3F_0\cos\left[\Omega\left(t - \frac{n_{\rm pl}}{c}x\right)\right]\right\}. \quad (3)$$

Here, $F_0 = (2/Z)^3 E_{\rm L}/E_{\rm A}$ is the normalized amplitude of the optical field, $E_{\rm A} = 5.14\cdot 10^9$ V/cm is the atomic unit of the electric field, $\hbar$ is Planck's constant, and Z is the charge number of ions (for C^{5+} ions), $Z = 6$. The third energy sublevel remains doubly degenerate and corresponds to the states $|4\rangle = |2p, m_{\rm mag} = 1\rangle$ and $|5\rangle = |2p, m_{\rm mag} = -1\rangle$. The energies of these states experience only the quadratic Stark effect and, as a result, a constant shift under the action of the modulating field: $\hbar\omega_4 = \hbar\omega_5 = -m_{\rm e}e^4Z^2(1 + 39F_0^2/8)/(8\hbar^2)$. Note that the ground state of the ions $|1\rangle = |1s\rangle$ also experiences some shift due to the quadratic Stark effect: $\hbar\omega_1(t,x) = -m_{\rm e}e^4Z^2(1 + 9F_0^2/256)/(2\hbar^2)$.

Dipole moments of the transitions $|2\rangle \leftrightarrow |1\rangle$ and $|3\rangle \leftrightarrow |1\rangle$ are oriented along the z axis, i. e., along the direction of polarization of fields (1) and (2). Accordingly, these transitions are excited by the resonant seeding radiation (2) and lead to its transformation in the medium. At the same time, the dipole moments of the transitions $|4\rangle \leftrightarrow |1\rangle$ and $|5\rangle \leftrightarrow |1\rangle$ are oriented perpendicular to the z axis. These transitions do not play any role in a resonantly absorbing medium, whereas they lead to the generation of amplified spontaneous radiation polarized along the y axis in an active medium.

Let us denote the lengths of the passive and active media as $L^{(\rm pas)}$ and $L^{(\rm act)}$, and their radii as R, where $R \ll \{L^{(\rm pas)}, L^{(\rm act)}\}$. Further, we assume that for X-ray radiation, the Fresnel numbers of each medium have the order of unity: $F^{(\rm pas)} = \pi R^2/[\lambda_{\rm inc}L^{(\rm pas)}] \sim 1$, $F^{(\rm act)} = \pi R^2/[\lambda_{\rm inc}L^{(\rm act)}] \sim 1$, where $\lambda_{\rm inc}$ is the wavelength of the seeding radiation (2). In this case, the propagation of resonant radiation in each medium is described with acceptable accuracy by a spatially one-dimensional wave equation.

A self-consistent system of quantum kinetic equations for the elements of the density matrix of a five-level medium and a wave equation for resonant radiation describing the transformation of seeding radiation in a modulated hydrogen-like medium is presented in [22–24]. This system takes into account the nonlinearity and dispersion of the medium (both plasma-based and resonant), as well as the generation of amplified spontaneous radiation in the active medium. However, in general, the system admits only a numerical solution. The results of simulations based on this system of equations are analyzed in Sec. 4.

3. ANALYTICAL SOLUTION

In order to get an analytical solution, we make additional approximations. We assume that the population of the resonance states of both active and passive media does not change, the amplified spon-

taneous radiation in the active medium can be neglected, and detuning of the seeding radiation (2) from the time-averaged frequency of the transitions $|2\rangle \leftrightarrow |1\rangle$ and $|3\rangle \leftrightarrow |1\rangle$ with allowance for the quadratic Stark effect, $\bar{\omega}_{\rm tr}^{(z)}$, is a multiple of twice the frequency of the modulating field: $\omega_{\rm inc} - \bar{\omega}_{\rm tr}^{(z)} = 2k^*\Omega$, where $\bar{\omega}_{\rm tr}^{(z)} \equiv 3m_{\rm e}e^4Z^2\,(1-109F_0^2/64)/(8\hbar^3)$, and k^* is an integer. In this case, the equations for the slowly varying amplitudes $\tilde{E}^{(z)}$ of X-ray radiation and the off-diagonal elements of the medium density matrix (quantum coherences) $\tilde{\rho}_{21}$ and $\tilde{\rho}_{31}$ take the following form:

$$\frac{\partial\tilde{E}^{(z)}}{\partial x} = i\frac{4\pi\bar{\omega}_{\rm tr}^{(z)}N_{\rm ion}d_{\rm tr}}{c\sqrt{\varepsilon_{\rm X-ray}}}(\tilde{\rho}_{21}-\tilde{\rho}_{31});$$
$$\frac{\partial\tilde{\rho}_{21}}{\partial\tau} = [-\gamma_{\rm tr} + i2k^*\Omega + i\Delta_{\rm L}\cos(\Omega\tau+\Delta Kx)]\tilde{\rho}_{21} - i\frac{d_{\rm tr}n_{\rm tr}}{2\hbar}\tilde{E}^{(z)};$$
$$\frac{\partial\tilde{\rho}_{31}}{\partial\tau} = [-\gamma_{\rm tr} + i2k^*\Omega - i\Delta_{\rm L}\cos(\Omega\tau+\Delta Kx)]\tilde{\rho}_{31} - i\frac{d_{\rm tr}n_{\rm tr}}{2\hbar}\tilde{E}^{(z)}. \quad (4)$$

Here, $\tau \equiv t - x\sqrt{\varepsilon_{\rm X-ray}}/c$ is the local time, $\varepsilon_{\rm X-ray}$ is the dielectric permittivity of the plasma at the frequency of the seeding radiation (2), $d_{\rm tr}$ is the absolute value of the dipole moment of the transitions $|2\rangle \leftrightarrow |1\rangle$ and $|3\rangle \leftrightarrow |1\rangle$, $n_{\rm tr}$ is the population difference at these transitions, $\Delta_{\rm L} = 3m_{\rm e}e^4Z^2F_0/(8\hbar^3)$ is the modulation amplitude of the frequencies of these transitions due to the linear Stark effect, $\gamma_{\rm tr}$ is the relaxation rate of resonant polarization of the medium, which allows for spontaneous radiation, collisions in the plasma, and ionization from the states $|2\rangle$ and $|3\rangle$ under the action of the modulating field, and $\Delta K = \Omega(\sqrt{\varepsilon_{\rm X-ray}} - n_{\rm pl})/c$ is the difference between the wave numbers of the modulating and resonant fields due to the dispersion of the plasma in the considered (passive or active) medium. Note that when deriving Eqs. (4), the resonant approximation ("rotating wave approximation") is also used and the terms oscillating at the double frequency of X-ray radiation are discarded. The carrier frequency for the field in the medium and the quantum coherence is chosen to be equal to the seeding radiation frequency $\omega_{\rm inc}$.

Next, we assume that the seeding radiation is monochromatic, $\tilde{E}_{\rm inc}(t) = E_{\rm inc}$, where $E_{\rm inc}$ does not depend on time, and we search for a steady-state solution for the field and off-diagonal elements of the medium density matrix. Let us represent the field in the medium as a Fourier series expansion,

$$\tilde{E}^{(z)} = \sum_{n=-\infty}^{+\infty} E_n\exp(-i2n\Omega\tau), \quad (5)$$

where $E_n = E_n(x)$ are the time-constant amplitudes of the combination spectral components. Then the solution for the slowly varying amplitude of the off-diagonal element of the medium density matrix $\tilde{\rho}_{21}$ will take the form

$$\tilde{\rho}_{21} = -i\frac{d_{\rm tr}n_{\rm tr}}{2\hbar}\sum_{n,\,m,\,k=-\infty}^{+\infty} E_nJ_m(P_\Omega)J_k(P_\Omega)\exp[i\,(k-m)\Delta K\,x]\frac{\exp[-i\,(m-k+2n+2k^*)\Omega\tau]}{\gamma_{\rm tr} - i\,(m+2n+2k^*)\Omega}, \quad (6)$$

where $J_n(P_\Omega)$ is an nth-order Bessel function of the first kind and $P_\Omega = \Delta_{\rm L}/\Omega$ is the modulation index (the ratio of the amplitude of the shift of resonant excited energy levels as a result of the linear Stark effect to the frequency of the modulating field). In a similar way, for the quantity $\tilde{\rho}_{31}$ we get

$$\tilde{\rho}_{31} = i\frac{d_{\rm tr}n_{\rm tr}}{2\hbar}\sum_{n,\,m,\,k=-\infty}^{+\infty} E_n(-1)^{m-k}J_m(P_\Omega)J_k(P_\Omega)\exp[i\,(k-m)\Delta K\,x]\frac{\exp[-i\,(m-k+2n+2k^*)\Omega\tau]}{\gamma_{\rm tr} - i\,(m+2n+2k^*)\Omega}. \quad (7)$$

We substitute the obtained expressions into the first equation of system (4) and take into account that the rates of onset of coherences $\tilde{\rho}_{21}$ and $\tilde{\rho}_{31}$ are much less than the frequency of the optical field: $\gamma_{\rm tr}/\Omega \ll 1$. This condition makes it possible to neglect the values of non-zero orders of smallness in the parameter $\gamma_{\rm tr}/\Omega$ in sums (6) and (7) and corresponds, first of all, to the neglect of the resonant dispersion of the medium at

the combination frequencies $\bar{\omega}_{\rm tr}^{(z)} \pm 2n\Omega$ (the resonant absorption at these frequencies is of a higher order of smallness in $\gamma_{\rm tr}/\Omega$). The approximations provide equations for the amplitudes of the spectral components of field (5) in the medium:

$$\frac{{\rm d}E_n}{{\rm d}x} = g_0 J_{2(n+k^*)}^2(P_\Omega) E_n(x) + g_0 J_{2(n+k^*)}(P_\Omega) \sum_{p=-\infty,\, p\neq 0}^{+\infty} E_{n+p}(x) J_{2(p+n+k^*)}(P_\Omega) \exp(i2p\,\Delta K\, x), \quad (8)$$

where $g_0 = 4\pi\bar{\omega}_{\rm tr}^{(z)} N_{\rm ion} n_{\rm tr} d_{\rm tr}^2/(\hbar c \gamma_{\rm tr}\sqrt{\varepsilon_{\rm X-ray}})$ is the coefficient of resonant amplification (if $g_0 > 0$) or absorption (if $g_0 < 0$). All the arguments up to now have been equally applied to both resonantly absorbing and amplifying media. Further, we consider each case separately.

The solution of Eqs. (8) is determined by two dimensionless parameters, namely, the modulation index P_Ω and the ratio of the resonant interaction coefficient to the addition to the difference in the wave numbers of the modulating and resonant fields due to plasma dispersion: $\alpha = |g_0|/(2\Delta K)$. In a resonantly absorbing medium modulated by a laser field of the visible or near/middle infrared spectral range with the parameters considered, the coefficient $\alpha \gg 1$. First of all, this is due to the fact that in the absorbing medium $n_{\rm tr} = -1$, and g_0 in absolute value is at least four times greater than in the inverted medium with an equally probable excitation of the states $|2\rangle$—$|5\rangle$ (in the latter case, $n_{\rm tr} \leq 1/4$). In addition, both the absolute and relative number densities of free electrons are significantly lower in a resonant absorber. As a result, the condition $2p\Delta K x \ll \pi$ is fulfilled for all significant p if the thickness is small enough. This condition makes it possible to neglect the exponent on the right-hand side of Eqs. (8). Herein, equalities that are valid for any value of $n \neq 0$ follow from Eqs. (8):

$$J_{2(n+k^*)}(P_\Omega) E_0 - J_{2k^*}(P_\Omega) E_n = C_n, \quad (9)$$

where C_n are constants. Equations (9) permit one to express E_n through E_0, after which the system of equations (8) for a non-dispersive medium, $\Delta K x \approx 0$, is reduced to the equation for the zero spectral component:

$$\frac{{\rm d}E_0}{{\rm d}x} = g_0 \sum_{n=-\infty}^{+\infty} J_{2(n+k^*)}^2(P_\Omega) E_0(x) + g_0 J_{2k^*}(P_\Omega) \sum_{n=-\infty,\, n\neq 0}^{+\infty} J_{2(n+k^*)}^2(P_\Omega) C_n, \quad (10)$$

and the system of equations (9). Using the substitution $E_0 = a_0(x)\exp[g_0 x \sum_{m=-\infty}^{+\infty} J_{2m}^2(P_\Omega)]$ it is possible to obtain a general solution to Eqs. (9) and (10) in the form

$$E_0 = C_0 \exp\left[g_0 x \sum_{m=-\infty}^{+\infty} J_{2m}^2(P_\Omega)\right] - J_{2k^*}(P_\Omega) \sum_{m=-\infty,\, m\neq 0}^{+\infty} J_{2(m+k^*)}^2(P_\Omega) C_m \Bigg/ \sum_{m=-\infty}^{+\infty} J_{2m}^2(P_\Omega),$$

$$E_n = \frac{J_{2(n+k^*)}(P_\Omega)}{J_{2k^*}(P_\Omega)} E_0 + J_{2(n+k^*)}(P_\Omega) C_n, \quad n \neq 0, \quad (11)$$

where the constants C_0 and C_n are determined by the boundary conditions. In the case under consideration, $E_0(x=0) = E_{\rm inc}$ and $E_n(x=0) = 0$ for $n \neq 0$. In this case,

$$C_0 = E_{\rm inc} \frac{J_{2k^*}^2(P_\Omega)}{\sum_{m=-\infty}^{+\infty} J_{2m}^2(P_\Omega)}, \qquad C_n = -\frac{E_{\rm inc}}{J_{2k^*}(P_\Omega)}.$$

Accordingly, the desired partial analytical solution of the system of equations (9) and (10), which satisfies the boundary conditions (2) and is valid for arbitrary values of x and P_Ω, has the form

$$E_0 = E_{\rm inc} \frac{J_{2k^*}^2(P_\Omega)}{S_{\rm even}(P_\Omega)} \exp[-S_{\rm even}(P_\Omega)\,|g_0|x_{\rm p}] + E_{\rm inc}\left[1 - \frac{J_{2k^*}^2(P_\Omega)}{S_{\rm even}(P_\Omega)}\right],$$

$$E_n = E_{\text{inc}} \frac{J_{2k^*}(P_\Omega) J_{2(n+k^*)}(P_\Omega)}{S_{\text{even}}(P_\Omega)} \exp[-S_{\text{even}}(P_\Omega)\,|g_0|x_{\text{p}}] - E_{\text{inc}} \frac{J_{2k^*}(P_\Omega) J_{2(n+k^*)}(P_\Omega)}{S_{\text{even}}(P_\Omega)}, \quad n \neq 0. \tag{12}$$

Here, $S_{\text{even}}(P_\Omega) = \sum_{m=-\infty}^{+\infty} J_{2m}^2(P_\Omega)$, x_{p} is the length of the propagation path in the absorber, $0 \le x_{\text{p}} \le L^{(\text{pas})}$, and it is taken into account that $g_0 < 0$ in a passive medium. Note that $S_{\text{even}}(0) = 1$ and $S_{\text{even}}(P_\Omega) \approx 1/2$ up to several tens of percent at $P_\Omega \ge 1$. It follows from this solution that in the absence of plasma dispersion, the resonant radiation in the medium is determined by the sum of two terms. The first of them corresponds to the absorbed multi-frequency structure of the field, and the second corresponds to a slightly different multi-frequency structure that propagates in the medium without absorption. Hereafter we call this structure the "transparent mode" of the field. The obtained solution provides fundamentally new information about the process of pulse formation in a passive medium compared to the previous paper [26]. Namely, the solution shows that in an optically thick medium, when the condition $S_{\text{even}}(P_\Omega)|g_0|x_{\text{p}} \gg 1$ is met, the field is determined by the "transparent mode" (see papers on the transparency of a modulated resonant absorber for multi-frequency radiation [29, 30]), and the characteristics of the field are insensitive to changes in the absorber thickness. Moreover, in contrast to the previous paper [26], solution (12) enables one to evaluate not only the spectral and temporal, but also the energy characteristics of resonant radiation in the medium. At the same time, solution (12) gives the same values of the relative amplitudes and phases of the combination spectral components as the simplified analytical solution obtained in [26] without allowance for the scattering of combination components. Accordingly, the analysis [26] of optimal conditions for the formation of pulses from the quasi-monochromatic seeding radiation remains topical.

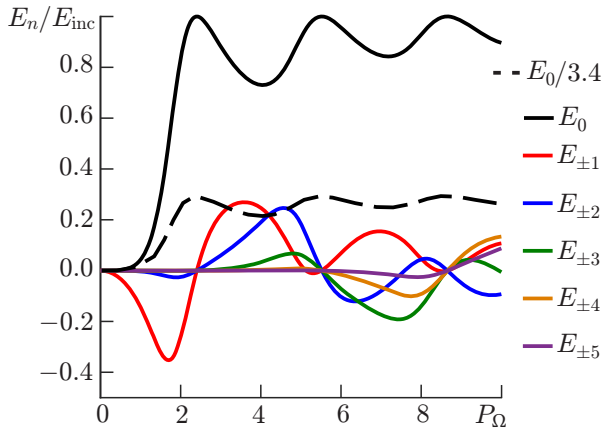

Fig. 1. Amplitudes E_n of the spectral components of the resonant radiation; the amplitudes are normalized by the amplitude E_{inc} of the seeding radiation at the output of an optically thick ($L^{(\text{pas})} = 1$ mm) absorber, depending on the modulation index P_Ω at $k^* = 0$ (the seeding radiation is in resonance with the modulated transition). The dependences are plotted in accordance with analytical solution (12).

As follows from solution (12), the spectral composition of the "transparent mode" is determined by the detuning of the seeding radiation from the time-average frequency of the resonant transition (the quantity k^*), as well as by the modulation index P_Ω (i. e., the amplitude and frequency of the modulating field). Figure 1 shows the dependences of the amplitudes of the combination spectral components of X-ray radiation at the output of an optically thick absorber ($|g_0|\,L^{(\text{pas})} = 45.8$, which corresponds to the absorber thickness $L^{(\text{pas})} = 1$ mm) on the modulation index P_Ω at $k^* = 0$ (the seeding radiation is in resonance with the modulated transition). It follows from this figure that the medium is opaque to resonant radiation in the absence of modulation ($P_\Omega \to 0$). As the modulation index is increased, the resonant absorber becomes a source of combination spectral components at frequencies $\bar{\omega}_{\text{tr}}^{(z)} \pm 2n\Omega$. In this case, i) the amplitudes of these components are real numbers, ii) the amplitude of the nth component reaches its maximum in absolute value at $P_\Omega \approx n$, and iii) the amplitudes of the components that differ only in the sign of the order n are equal to each other, i. e., $E_n = E_{-n}$.

Then we consider the value of the modulation index $P_\Omega = 4.2$, which is optimal for both the resonant absorber and the active medium (see the discussion after Eqs. (13)). Herein, five components dominate in the X-ray spectrum in a passive medium: the amplitude of the central component is close to the local minimum, $E_0 \approx 0.73E_{\text{inc}}$, while the amplitudes of the nearest combination components are equal to each other and close to the maximum, namely, $E_{\pm1} \approx E_{\pm2} \approx 0.22E_{\text{inc}}$, and the components of the higher orders do not play a notable role: $E_{\pm3} \approx 0.04E_{\text{inc}}$ and $E_{\pm n} < 0.01E_{\text{inc}}$ for $n \ge 4$. For the chosen value of the modulation index, all the spectral components of the field are in phase and form a sequence of spectrally limited pulses

in the time domain, which are shown in Fig. 2. Figure 2 also shows the intensity of X-ray radiation after the attenuation of the central component of the radiation spectrum to the level of combination frequencies (by a factor of 3.4 in amplitude). It follows from this figure that spectral filtering significantly improves the pulse shape and reduces the pulse duration from $0.096T$ to $0.078T$, where $T = 2\pi/\Omega$ is the period of the modulating field, but decreases their peak intensity from $2.9I_{\rm inc}$ to $1.4I_{\rm inc}$, where $I_{\rm inc} = c|E_{\rm inc}|^2/(8\pi)$ is the intensity of the seeding radiation. In practice, the attenuation of the central spectral component of the field can be achieved using spectrally selective multilayer X-ray mirrors, see [31, 32].

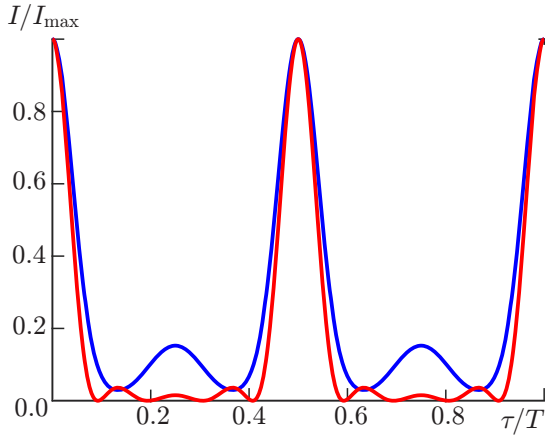

Fig. 2. Time dependence of the intensity of the resonant radiation transformed in a modulated absorber for $P_\Omega = 4.2$, $k^* = 0$, and $L^{(\rm pas)} = 1$ mm, which corresponds to Eq. (12). The intensity is normalized to its peak value $I_{\rm max}$ for each curve. The blue solid curve corresponds to the field after the absorber ($I_{\rm max} = 2.9I_{\rm inc}$, $I_{\rm inc}$ is the intensity of the seeding radiation) and the red curve, to the case with additional attenuation of the central component of the field spectrum by 3.4 times ($I_{\rm max} = 1.4I_{\rm inc}$). The local time τ is normalized by the period of the modulating field $T = 2\pi/\Omega$.

The X-ray radiation transformed in a modulated resonant absorber is delivered to the entrance of the amplifying active medium irradiated by the same optical field. As is shown in [22, 25], the spectral components of the field of different orders are amplified independently from each other in an active medium with a high number density of free electrons. This conclusion directly follows from Eqs. (8): when the condition $\alpha = |g_0|/(2\Delta K) \ll 1$ is fulfilled, the inverse of what was used in the derivation of solution (12), the sum on the right-hand side of Eqs. (7) is a rapidly oscillating (on the scale of the characteristic amplification length) alternating function of the x coordinate. As a result, the contribution of the function to the solution is insignificant. In this case, each spectral component of the resonant radiation is amplified independently from the other components with a gain proportional to the square of the Bessel function of the corresponding order: $E_n \propto \exp[g_0 J_{2n}^2(P_\Omega)x]$, where $g_0 > 0$. Thus, the dependences of the amplitudes of the spectral components of X-ray radiation (5), previously transformed in a resonant absorber with the thickness $L^{(\rm pas)}$, on the length of the propagation path in the active medium, $x = x_{\rm a}$, $0 \le x_{\rm a} \le L^{(\rm act)}$, take the form

$$E_0 = E_{\rm inc}\exp\left(g_{\rm eff(0)}^{(\rm act)}x_{\rm a}\right)\left\{\frac{J_{2k^*}^2(P_\Omega)}{S_{\rm even}(P_\Omega)}\left[\exp(-g_{\rm eff}^{(\rm pas)}L^{(\rm pas)})-1\right]+1\right\},$$
$$E_n = E_{\rm inc}\exp\left(g_{\rm eff(n)}^{(\rm act)}x_{\rm a}\right)\frac{J_{2k^*}(P_\Omega)J_{2(n+k^*)}(P_\Omega)}{S_{\rm even}(P_\Omega)}\left[\exp(-g_{\rm eff}^{(\rm pas)}L^{(\rm pas)})-1\right], \quad n \ne 0. \qquad (13)$$

Here, $g_{\rm eff(n)}^{(\rm act)}(P_\Omega) \equiv J_{2n}^2(P_\Omega)g_0^{(\rm act)}$ is the gain rate of the nth spectral component of the field in a modulated active medium and $g_{\rm eff}^{(\rm pas)}(P_\Omega) \equiv S_{\rm even}(P_\Omega)|g_0^{(\rm pas)}|$ is the decay rate of the multi-frequency field in a resonant absorber. For the considered modulation index, $P_\Omega = 4.2$, $J_0^2(4.2) = 0.1418$, $J_{\pm2}^2(4.2) = 0.0964$, and $J_{\pm4}^2(4.2) = 0.0961$. Accordingly, the combination components $n = \pm1$ and $n = \pm2$ in the resonant radiation spectrum are amplified uniformly, while the central component has the largest gain rate. As a result, during the amplification process, the inequality of the amplitudes of the central and sideband spectral components of the radiation increases, which leads to the need for additional attenuation of the central component. Note that the chosen value of the modulation index provides the most uniform amplification of the spectral components of X-ray radiation in the range $2.4 \le P_\Omega \le 5.1$, which is optimal for the formation of pulses in a modulated absorber from the resonant seeding radiation [26].

The dependence of the amplitudes of the spectral components of the field (13) on the modulation

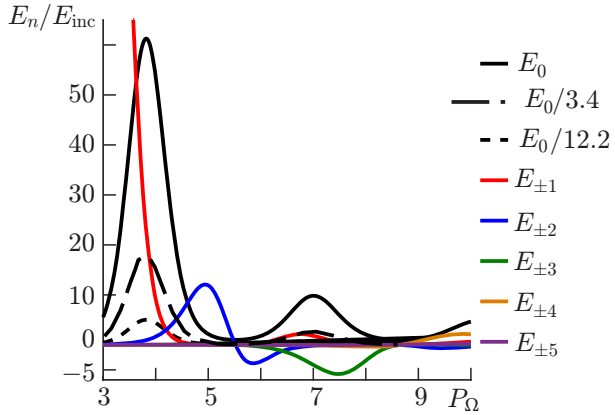

Fig. 3. The amplitudes E_n of spectral components of the resonant radiation, which correspond to Eqs. (13) and are normalized to the amplitude $E_{\rm inc}$ of the seeding radiation, at the output of the combination of an absorber with the thickness $L^{(\rm pas)} = 1$ mm and an active medium with the thickness $L^{(\rm act)} = 0.5$ mm, modulated by the same optical field, as functions of the modulation index P_Ω when $k^* = 0$ (the seeding radiation is in resonance with the modulated transition).

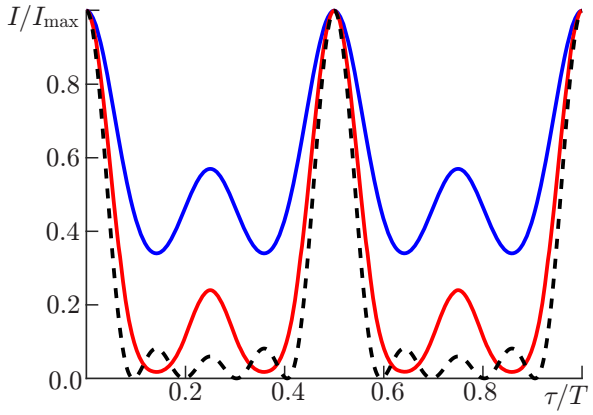

Fig. 4. Time dependence, corresponding to Eqs. (13), of the intensity of the radiation transformed into combinations of a resonant absorber with the thickness $L^{(\rm pas)} = 1$ mm and an active medium with the thickness $L^{(\rm act)} = 0.5$ mm, modulated by the same optical field, for $P_\Omega = 4.2$ and $k^* = 0$. The intensity is normalized to its peak value $I_{\rm max}$ for each curve. The blue solid curve characterizes the field without spectral filtering ($I_{\rm max} = 2014 I_{\rm inc}$), the red curve implies attenuation of the central component of the field spectrum by 3.4 times ($I_{\rm max} = 465 I_{\rm inc}$), and the black dotted curve corresponds to attenuation of the central spectral component by 12.2 times ($I_{\rm max} = 212 I_{\rm inc}$).

index is shown in Fig. 3. In this figure, the optical thickness of the active medium was assumed to be equal to $g_0^{(\rm act)} L^{(\rm act)} \approx 27$, which in the case of a 100% population inversion at the transition $n_{\rm pr} = 1 \leftrightarrow n_{\rm pr} = 2$ (the probability of detecting ions in each state $|2\rangle \leftrightarrow |5\rangle$ is 1/4 in this case) for a medium with the ion density C^{5+} $N_{\rm ion}^{(\rm act)} = 10^{19}\,{\rm cm}^{-3}$ corresponds to a medium thickness of 0.5 mm. Note that the effective optical thickness for each spectral component of the field is an order of magnitude smaller than $g_0^{(\rm act)} L^{(\rm act)}$ due to the smallness of the Bessel functions squared. In Fig. 3, the amplitude of the central component of the field spectrum is shown for three cases, namely, without attenuation, with attenuation by 3.4 times, which is optimal for the formation of pulses in a passive medium, and with attenuation by 12.2 times, which is optimal for an active medium of the considered thickness.

Figure 4 shows the corresponding time dependences of the X-ray radiation intensity on the scale of the optical field period. If the central component of the spectrum is not attenuated, then the pulses are formed against the background of an intense pedestal. Note that the level of the pulse pedestal decreases when a medium with a lower optical thickness is used, and this option can also be of interest. At the same time, as in a passive medium, the attenuation of the central component of the field spectrum significantly improves the shape of the pulses and reduces their duration due to a decrease in the peak intensity.

Note that in accordance with the analytical solution (12), (13) and in consistence with [26], pulses can also be formed from the seeding radiation separated from the resonance with the absorber by ± 2 frequencies of the modulating field ($k^* = \pm 1$). In this case, the optimal modulation index for the combination of a resonant absorber and an active medium is $P_\Omega \approx 6.4$. At the output of the resonant absorber, the field spectrum contains seven components with significantly non-zero amplitudes, one of which ($n = -2$ for $k^* = 1$ and $n = +2$ for $k^* = -1$) is antiphase to the others. However, the presence of an antiphase component does

not preclude the formation of pulses after the modulated absorber when the central component of the field spectrum is attenuated by 5.5 times in amplitude. The shape of the pulses corresponds to Fig. 7 from [26], and the duration turns out to be less by 20–30% than in the case $P_\Omega = 4.2$ where a modulating field with the same wavelength is used. However, in the process of amplification in the active medium, the role of the antiphase spectral component of the field increases due to the unequal gains for the different-order spectral components. As a result, the formation of pulses is possible only after a significant attenuation (suppression) of the antiphase component.

In the next section, the obtained conclusions of the analytical theory are compared with the results of numerical simulation, which takes into account the nonlinearity and both the resonant and plasma dispersion of each medium, as well as the generation of amplified spontaneous radiation from the quantum noise of the active medium.

4. THE RESULTS OF NUMERICAL SIMULATION

This section of the paper analyzes the results of numerical simulations based on a self-consistent system of Maxwell–Bloch equations for resonant radiation and a sequence of five-level hydrogen-like media (passive and active) with quantum transition frequencies variable in time and space. This system of equations and methods of its solution are described in detail in [22–24]. The analytical solution is obtained in the approximation of the monochromatic seeding radiation with a time-constant amplitude, $\tilde{E}_{\rm inc}(t) = E_{\rm inc}$, while this section considers the seeding radiation with an envelope of the form

$$\tilde{E}_{\rm inc}(t) = \begin{cases} E_{\rm inc}\sin^2\left(\pi\dfrac{\Delta\tau_0 - \tau}{\Delta\tau_0}\right), & 0 \le \tau \le \Delta\tau_0; \\ 0, & \tau < 0, \quad \tau > \Delta\tau_0. \end{cases} \tag{14}$$

Here, $\Delta\tau_0$ is the duration of the seeding radiation from zero to zero, while the duration at the half-height of the intensity is $\Delta\tau_{1/2} \approx \Delta\tau_0/2.74$. In numerical simulations, the quantity $\Delta\tau_0$ plays a significant role due to the resonant dispersion (the finite time of onset of the resonant response) of each medium, as well as a decrease in the population inversion in the active medium over time as a result of spontaneous and forced transitions.

As was mentioned earlier, we assume that the number densities of resonant ions and free electrons in the passive medium are $N_{\rm ion}^{\rm (pas)} = 10^{17}\,{\rm cm}^{-3}$ and $N_{\rm e}^{\rm (pas)} = 5\cdot 10^{17}\,{\rm cm}^{-3}$, respectively. For the electron temperature $T_{\rm e} \approx 5$ eV and ion temperature $T_{\rm ion} \approx 3\,{\rm eV}$, which are similar to the parameters of the active medium with the same number density of ions and electrons [21] (this estimate of the plasma temperature seems reasonable if the active and passive media are created in the same way), the average time between particle collisions in the plasma absorber will be $1/\gamma_{\rm coll}^{\rm (pas)} = 560$ fs. Note that varying the temperature of particles in the absorber several times will not change the basic properties of the solutions discussed below. In an active medium with the ion number density $N_{\rm ion}^{\rm (act)} = 10^{19}\,{\rm cm}^{-3}$ and electron number density $N_{\rm e}^{\rm (act)} = 1.5\cdot 10^{20}\,{\rm cm}^{-3}$, this value is much less, $1/\gamma_{\rm coll}^{\rm (act)} = 20$ fs [22]. Further, we assume that both media are irradiated by a laser field with the intensity $I_{\rm L} = 2.3\cdot 10^{16}\,{\rm W/cm}^2$ close to the threshold of rapid ionization from the resonant excited states of C^{5+} ions. In this case, the characteristic time of ionization from the states $|2\rangle$ and $|3\rangle|$ is $1/w_{\rm ion}^{(2,3)} = 2.3$ ps. With allowance for the ionization, the relaxation time of quantum coherence (off-diagonal elements of the density matrix) in the resonant absorber is $1/\gamma_{\rm tr}^{\rm (pas)} = 450$ fs. In the active medium, the relaxation of quantum coherence is also caused by spontaneous transitions of ions from excited states to the ground state with rate $\Gamma_{\rm rad}$, where $1/\Gamma_{\rm rad} = 1.23$ ps. In view of the fact that $\Gamma_{\rm rad} \ll \gamma_{\rm coll}^{\rm (act)}$ and $w_{\rm ion}^{(2,3)} \ll \gamma_{\rm coll}^{\rm (act)}$, in an active medium with considered parameters we have $1/\gamma_{\rm tr}^{\rm (act)} \approx 1/\gamma_{\rm coll}^{\rm (act)} = 20$ fs. Accordingly, $1/\gamma_{\rm tr}^{\rm (pas)} \gg 1/\gamma_{\rm tr}^{\rm (act)}$, and the onset of resonant polarization in the absorber is much slower than in the active medium. As a result, if the duration $\Delta\tau_0$ of the seeding radiation is comparable to or less than $1/\gamma_{\rm tr}^{\rm (pas)}$, then the expansion of the resonant radiation spectrum, as well as the absorption of

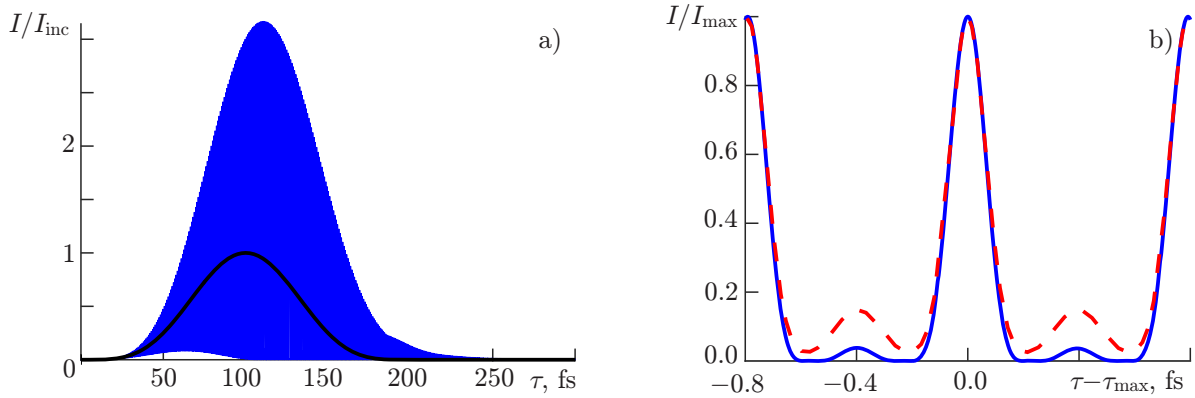

Fig. 5. Panel *a*: time dependence of the X-ray intensity at the output of an absorber with the thickness $L^{(\text{pas})} = 1$ mm (blue curve), as well as at the input to the medium (black curve). The intensity is normalized to the peak intensity $I_{\text{inc}} = 10^{12}\,\text{W/cm}^2$ of the seeding radiation. Panel *b*: the shape of pulses at the maximum of the envelope of the pulse sequence of panel *a* (blue curve) and the result of analytical solution (12) (red dotted line). The intensity is normalized to the peak pulse intensity $I_{\max} = 3.2I_{\text{inc}}$ for the numerical solution and $I_{\max} = 2.9I_{\text{inc}}$ for the analytical solution. The position of the maximum of the envelope of the output radiation is $\tau_{\max} \approx 110$ fs and the pulse duration is $\tau_{\text{pulse}} = 150$ as.

its central component, occur with a certain delay relative to the leading edge of the signal. This effect decreases with increasing optical thickness of the medium, $g_{\text{eff}}^{(\text{pas})} L^{(\text{pas})}$, but as its physical thickness $L^{(\text{pas})}$ is increased, the plasma dispersion effect also increases and the conditions for the applicability of analytical solutions (12) and (13) are violated. Thus, the efficiency of expansion of the seeding radiation spectrum in a passive medium increases with increasing radiation duration $\Delta\tau_0$. At the same time, in an active medium with considered initial conditions (at $\tau = 0$ all ions are excited), the population difference monotonically decreases with increasing local time as a result of spontaneous and forced transitions. If spontaneous radiation (which occurs in all directions, not only along the axis of the plasma channel, but also into an angle of 4π steradians) dominates, then the population difference reverses sign at $\tau = \tau_{\text{zero}} \approx 270$ fs [24]. With allowance for stimulated radiation, the depletion of excited states is accelerated. Accordingly, in order to provide signal amplification, the duration of the seeding radiation should be less than the lifetime of the population inversion in the active medium, $\Delta\tau_0 < \tau_{\text{zero}}$, and the amplification will be greater, the better this inequality is fulfilled.

In what follows, the results of numerical simulations for $\Delta\tau_0 = 200$ fs ($\Delta\tau_{1/2} = 73$ fs) are presented and the results of simulations for $\Delta\tau_0 = 100$ fs ($\Delta\tau_{1/2} = 36.5$ fs) are also discussed. Note that the indicated durations of the X-ray seeding radiation correspond to the characteristic values achieved in the high-order harmonic generation experiments. The wavelength of the seeding radiation tuned to a resonance with modulated transition is $\lambda_{\text{inc}} = 3.37$ nm. The peak intensity of the seeding radiation is chosen to be equal to $I_{\text{inc}} = 10^{12}\,\text{W/cm}^2$. The wavelength of the modulating field in free space is assumed to be equal to $\lambda_{\text{L}} = 2\pi c/\Omega = 472$ nm. For this wavelength and the chosen laser radiation intensity, $I_{\text{L}} = 2.3 \cdot 10^{16}\,\text{W/cm}^2$, the modulation index is $P_\Omega = 4.2$. At the same time, the results presented below can be qualitatively reproduced if a modulating field with a longer (up to a few microns) wavelength is used and its amplitude is decreased proportionately. In this case, the modulation index will be fixed, and the pulse duration and repetition period will increase in proportion to the wavelength of the modulating field.

Figure 5 shows the time dependence of the X-ray radiation intensity at the output of an absorber with the thichness $L^{(\text{pas})} = 1$ mm (the effective optical thickness of the absorber is $g_{\text{eff}}^{(\text{pas})} L^{(\text{pas})} = 24.24$), as well as the intensity of the seeding radiation. It can be seen in this figure that a sequence of pulses with a duration and peak intensity equal to 150 as and $3.2I_{\text{inc}}$, respectively, at the maximum of the envelope is formed as a result of propagation in the medium. The formation of pulses is achieved due to the redistribution of the seeding radiation energy over combination frequencies and their constructive interference in the time domain. At the same time, the time-average intensity of the resonant radiation decreases with increasing thickness

of the absorber. Due to the finite response time of the absorber, a pedestal is formed at the leading edge of the formed pulse sequence due to the dominance of the central component in the signal spectrum, and the position of the envelope maximum is shifted to longer times relative to the seeding radiation maximum. In this case, the peak intensity of the pulses is higher, and the shape is better than in the analytical solution, which is due to a slightly different spectrum of the transformed radiation.

The dependences of the amplitudes of the spectral components of the resonant radiation on the absorber thickness are shown in Fig. 6. This figure also shows the results of the analytical solution (12). At a small thickness, the numerical solution qualitatively reproduces the results of the analytical theory: first, there is a rapid increase in the amplitudes of the combination spectral components and attenuation of the central component of the spectrum, and then the amplitudes of the spectral components reach a plateau and change only slightly as the absorber thickness is varied in the range $0.3\,\text{mm} \leq x_\text{p} \leq 0.7$ mm. With the further increase in the absorber thickness, the resonant radiation spectrum changes significantly due to plasma dispersion and reproduces some features of the analytical solution obtained for a highly dispersive medium [24]. Namely, the amplitudes of the combination components oscillate with the variation in the thickness of the medium, while the scale of variation in the amplitudes of the components $n = 1$ and $n = -1$ is twofold larger than that of the components $n = 2$ and $n = -2$. At the same time, coherent scattering of the sideband components into the central component of the spectrum leads to the fact that the amplitude of the central component significantly deviates from the analytical solution, vanishes when the medium is about 2 mm thick and then varies periodically with increasing thickness. As a result, the amplitudes of the spectral components of the resonant radiation are comparable to each other in a wide range of absorber thicknesses, and in some cases they are even closer to each other than in the analytical solution. Accordingly, the output radiation maintains the form of the sequence of pulses when the thickness of the medium is varied from 0.5 to 4.5 mm (see Fig. 7). Note that the results shown in Figs. 5–7 are generally reproduced when the duration of the seeding radiation is reduced from $\Delta\tau_0 = 200$ fs to $\Delta\tau_0 = 100$ fs. At the same time, the role of the delay of the resonant response (resonant dispersion) of the absorber increases: the pedestal of pulses at the leading edge of the signal increases, the peak intensity of the pulses decreases slightly, and the trailing edge of the signal significantly elongates with increasing thickness of the medium.

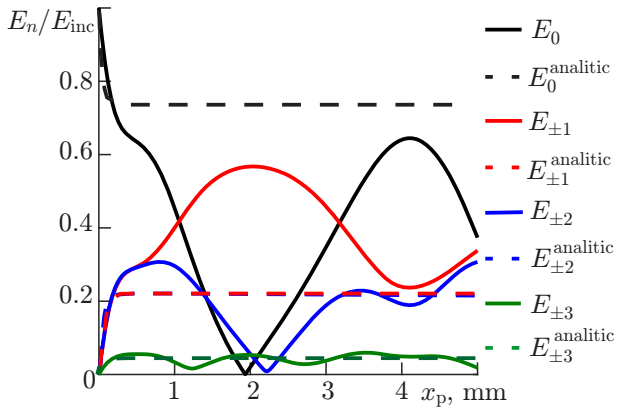

Fig. 6. Dependences of the amplitudes of the spectral components of the resonant radiation on the thickness of the absorber. The central component of the spectrum is shown in black. The red, blue, and green colors correspond to the combination components $n = \pm1$, $n = \pm2$, and $n = \pm3$. The solid lines show the results of the numerical solution and the dashed lines correspond to the analytical solution (12).

Next, we consider the amplification of the pulse sequence depicted in Fig. 5 in an active medium modulated by the same optical field. Figure 8 shows the time dependence of the intensity of the amplified radiation at the exit from of the medium with a thickness of 0.4 mm. The blue curve shows the radiation intensity directly after the combination of a resonant absorber and an active medium, while the red curve shows the radiation intensity after the additional attenuation of the central component of the radiation spectrum by three times (to the level of the combination components at the exit from the active medium). The green curve shows the intensity of the amplified spontaneous radiation of an active medium with y-polarization. Figure 8*a* shows the time dependences on a sub-picosecond scale, whereas Fig. 8*b* shows the shape of individual attosecond pulses at the maximum of the intensity envelope. As a comparison, the results of the analytical solution for a combination of passive and active media with the same parameters are also presented there. It can be seen in this figure that after the amplification, the peak intensity of a

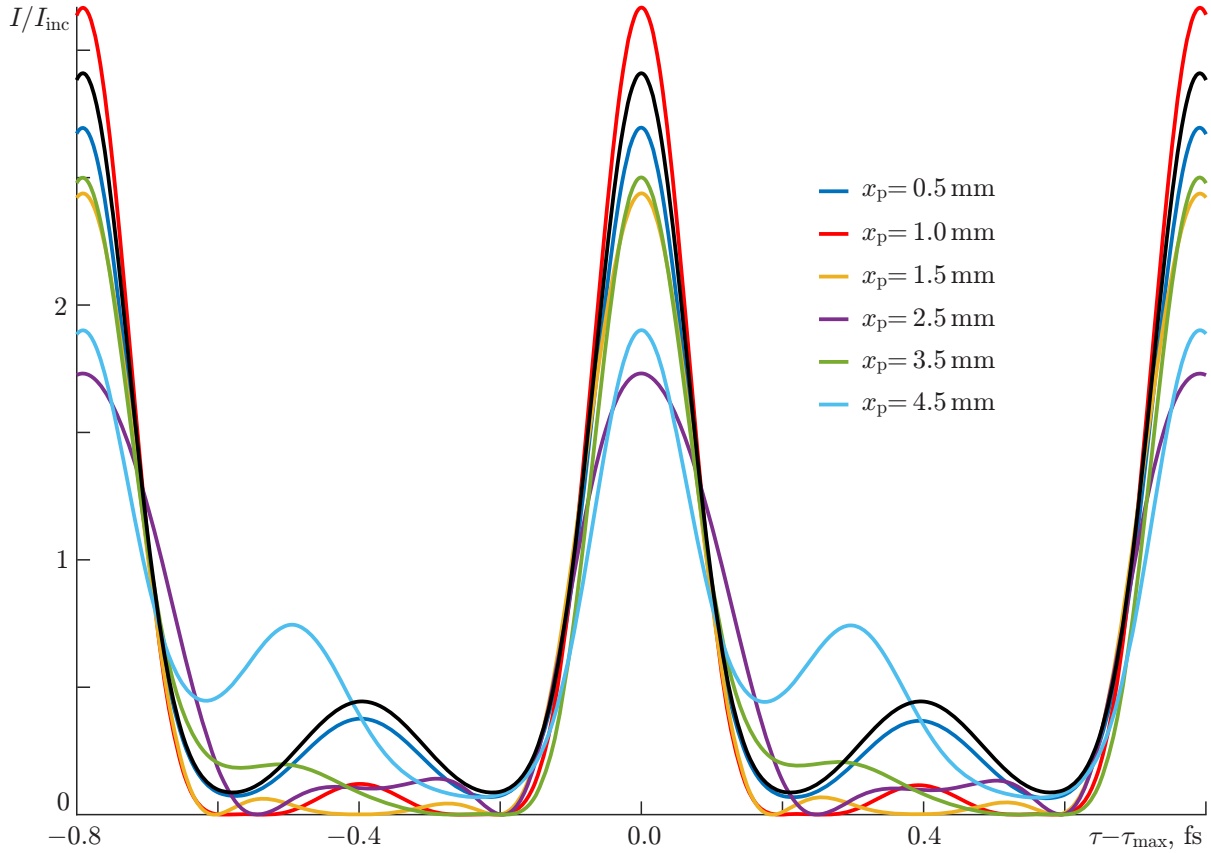

Fig. 7. Pulse shape at the maximum of the envelope of the transformed radiation as a function of the absorber thickness. The colored curves correspond to the results of the numerical solution, the black line shows the analytical solution (12). The intensity is normalized to the peak intensity I_{inc} of the seeding radiation. The position of the maximum of the envelope of the output radiation depends on the thickness of the medium and varies in the range 100 fs $< \tau_{\max} <$ 155 fs.

pulse is approximately 27 times higher than the intensity I_{inc} of the seeding radiation and is $2.7 \cdot 10^{13}$ W/cm^2 ($1.1 \cdot 10^{13}$ W/cm^2 in the case of attenuation of the central components of the spectrum), which is an order of magnitude greater than the intensity that can be achieved when the pulses are generated directly in the active medium of an X-ray laser (with the same value of I_{inc}) [24]. The pulse duration is 200 as (150 as when the central component of the spectrum is attenuated). Comparison of the pulse shape with the analytical solution shows that the latter greatly overestimates the amplification of the active medium (the peak intensity of the signal in the analytical solution reaches $5.1 \cdot 10^{14}$ W/cm^2), which leads to a greater inhomogeneity of the spectrum of the amplified radiation and a higher pedestal of the pulses generated. In reality, the amplification appears to be much weaker, primarily because of the rapid decrease in the population difference at the inverted ion transition due to spontaneous and forced transitions.

The spectral composition of the amplified radiation as a function of the thickness of the active medium, is plotted in Fig. 9. At the initial stage of amplification, the amplitudes of the combination components with $n = \pm 1$ and $n = \pm 2$ increase almost linearly as they propagate in the medium and increase twofold at $x_{\text{a}} = 0.4$ mm. At the same time, the growth of the central component of the field spectrum occurs faster (the central component increases in amplitude by 5.3 times when the thickness of the medium $x_{\text{a}} = 0.4$ mm) and appears nonlinear. However, with the further increase in the thickness of the medium, the amplitudes of the combination components start to decrease, and the growth of the amplitude of the central component slows down. This effect is due to two reasons. First, at the entrance to the active medium, the radiation is spectrally inhomogeneous as a result of the delay in the resonant response of the absorber to the seeding

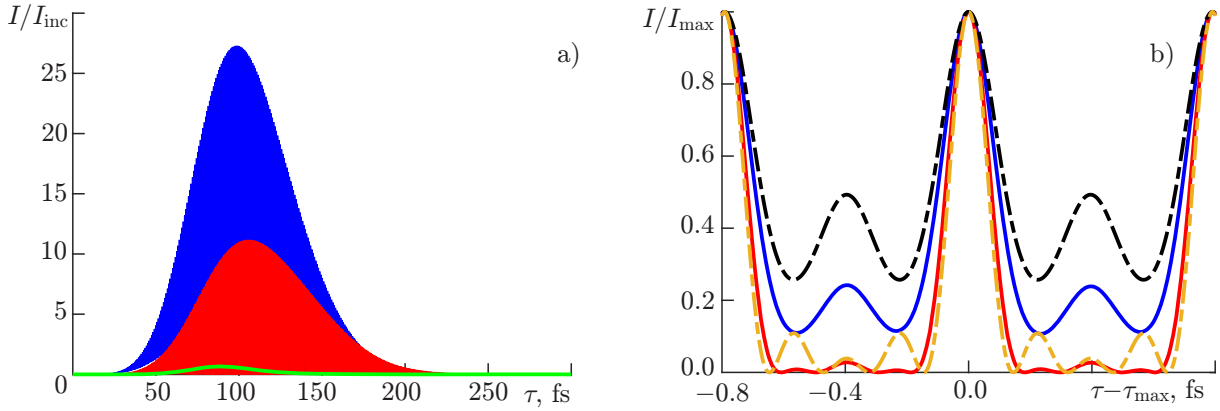

Fig. 8. Panel *a*: time dependence of the intensity (normalized to the peak intensity I_{inc} of the seeding radiation) of X-ray radiation after a sequentially arranged resonant absorber with the thickness $L^{(\text{pas})} = 1$ mm and an active medium with the thickness $L^{(\text{act})} = 0.4$ mm. The blue curve corresponds to the radiation intensity directly after the active medium, the red curve, to the radiation intensity after the central component of the spectrum has been attenuated threefold (to the level of the combination components), and the green curve, to the amplified spontaneous radiation of the active medium. Panel *b*: pulse shape at the maximum of the intensity envelope, $\tau \approx \tau_{\max}$, without (blue curve) and with (red curve) attenuation of the central component of the field spectrum. The results of the analytical solution for the same conditions are shown by black (without the attenuation) and orange (with the central component of the field spectrum attenuated to the level of the components with $n = \pm 1$, i. e., by 12.2 times) dashed dotted lines. The intensity is normalized to the peak intensity $I_{\max}$ of the pulses. In the numerical solution without spectral filtering, $I_{\max} = 27.3 I_{\text{inc}}$, $\tau_{\max} \approx 98$ fs, and the pulse duration $\tau_{\text{pulse}} = 200$ as. With attenuated central component of the spectrum, $I_{\max} = 11.2 I_{\text{inc}}$, $\tau_{\max} \approx 106$ fs, and the pulse duration $\tau_{\text{pulse}} = 150$ as.

radiation (14). As a result, the central component of the spectrum prevails at the leading edge of the incident (on the active medium) signal, while the combination components appear with a certain delay. Second, with the increase in the thickness of the active medium, the intensity of the amplified signal also increases, and the duration of the time interval, during which the amplification occurs, decreases due to the depletion of the excited states in the amplification process, after which the medium becomes absorbing (see Fig. 10). In total, these reasons lead to the fact that for a medium with the thickness $x_{\text{a}} \geq 0.5$ mm the absorption of the combination spectral components at the trailing edge of the amplified pulse sequence is more significant than their amplification at the leading edge of the signal. At the same time, the central component of the spectrum (integrally over the entire calculation time) continues to amplify, although not as effectively as in a medium with a smaller thickness. Note that the peak intensity of the pulses increases slightly with decreasing duration of the seeding radiation. Thus, at the transition from $\Delta\tau_0 = 200$ fs to $\Delta\tau_0 = 100$ fs the peak intensity of attosecond pulses increases to $3.5 \cdot 10^{13}\,\text{W/cm}^2$ for the same thickness of the medium. We also note that the small-scale structure on the spatial dependences of the amplitudes of the spectral components of the resonant radiation is due to their mutual scattering [25], which in this case is suppressed due to the high number density of free electrons.

The evolution of the pulse shape with increasing thickness of the active medium is shown in Fig. 11. As the thickness of the medium is increased, the level of the pedestal of the pulses also increases, and their duration rises slightly, while the pulse shape is preserved. Thus, the spectral–temporal characteristics of the pulses have a low sensitivity to changes in the optical thickness of the active medium in a wide range (from 0.1 mm to 1 mm).

To conclude this section, it should be noted that similar results can be obtained with lower intensities of the X-ray seeding radiation. Herein, the difference in the passive medium will be minimal, and the pulse amplification will be even more effective in the active medium due to the lower rate of depletion of excited states (the role of amplified spontaneous radiation will increase, see [22, 24]).

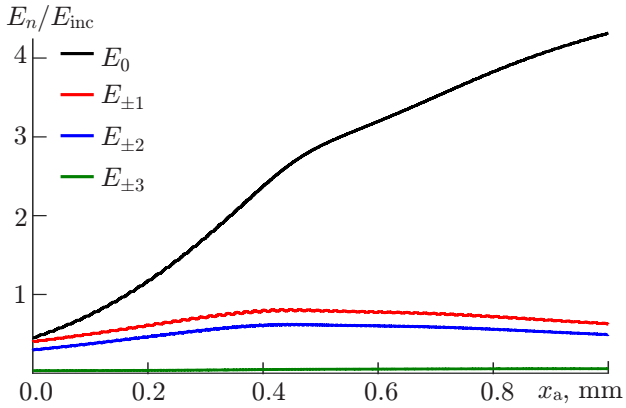

Fig. 9. Dependences of the amplitudes of the spectral components of the resonant radiation on the thickness of the active medium. The central component of the spectrum is shown in black. The red, blue, and green colors correspond to the combination components with $n = \pm1$, $n = \pm2$, and $n = \pm3$.

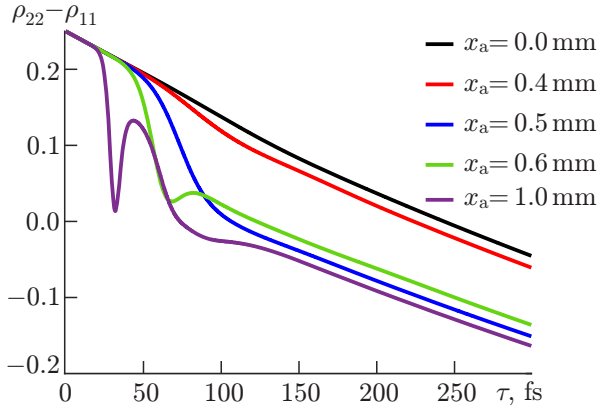

Fig. 10. The dependence of the population difference at the transition $|2\rangle \leftrightarrow |1\rangle$ of the active medium on the local time for different thicknesses of the medium x_a. At $x_a \leq 0.4$ mm, the decrease in the population difference is due mainly to the spontaneous radiation. For large thicknesses, the role of forced transitions increases due to increased spontaneous radiation of the active medium. The population differences at the transitions $|2\rangle \leftrightarrow |1\rangle$ and $|3\rangle \leftrightarrow |1\rangle$ coincide on the figure scale.

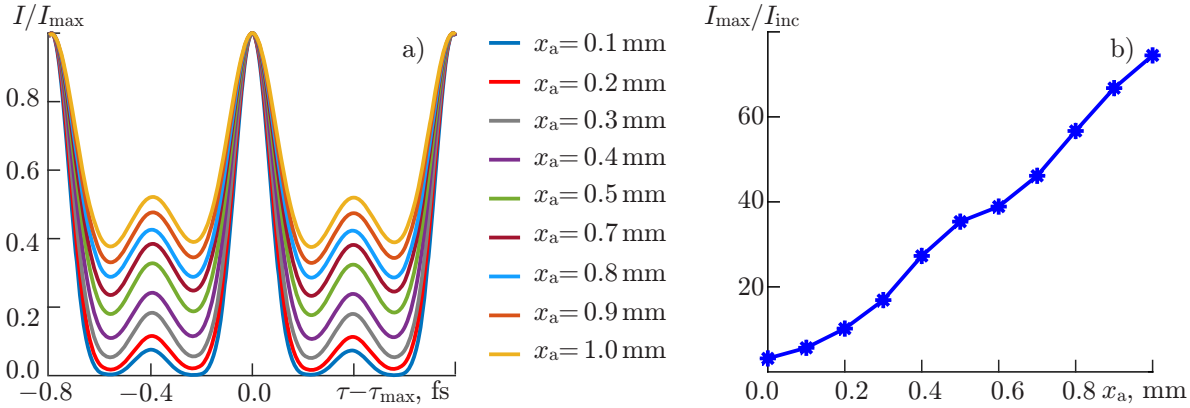

Fig. 11. Panel *a*: pulse shape at the maximum of the envelope of the transformed radiation as a function of the thickness x_a of the active medium. The intensity is normalized to the peak intensity $I_{\max}$ of the pulses. The maximum of the envelope of the pulse sequence is reached at the instant 73 fs $\leq \tau_{\max} \leq$ 110 fs, which differs for different thicknesses of the medium. Panel *b*: the peak pulse intensity $I_{\max}$ as a function of the thickness of the active medium.

5. CONCLUSIONS

We have proposed a new approach to the implementation of the method of formation and amplification of attosecond pulses in the active medium of a plasma-based X-ray laser irradiated by an intense laser field of the optical or infrared range [21, 22]. Namely, it is proposed to use the combination of a resonantly absorbing medium and a similar active medium of a plasma-based X-ray laser modulated by the same optical field to transform the quasi-monochromatic X-ray seeding radiation into a sequence of attosecond pulses. It is shown that the formation of pulses in this case occurs in a resonant absorber, and the role of the active medium consists in a subsequent amplification of the pulses. The parameters of both media can be optimized

accordingly to solve each of these problems. In this case, an order of magnitude higher radiation intensity is achieved with a better shape and comparable duration of attosecond pulses compared to their formation directly in the modulated active medium of a plasma-based X-ray laser [24]. In addition, it is shown that the pulse formation mode is insensitive to changes in the optical thickness of each medium over a wide range. The plasma of hydrogen-like C^{5+} ions with population inversion at the transition $n_{\text{pr}} = 1 \leftrightarrow n_{\text{pr}} = 2$ (n_{pr} is the main quantum number) is considered as resonantly absorbing and active media [27]. The wavelength of the resonant radiation (and the generated attosecond pulses) in this case is about 3.4 nm and lies in the "water window" range.

An analytical solution describing the transformation of the quasi-monochromatic seeding radiation in a resonant absorber and an active medium located one after the other has been obtained. The analytical solution shows that a multi-frequency "transparent mode" of resonant radiation is formed in a modulated absorber and propagates in the medium without absorption. The spectral–temporal characteristics of the "transparent mode" are determined by the modulating field, as well as by detuning of the seeding radiation from the resonance; under optimal conditions, they correspond to the formation of a sequence of spectrally limited attosecond pulses. In turn, in a modulated active medium, attosecond pulses are amplified with an approximate conservation of their duration and shape [22].

Based on analytical and numerical solutions, the possibility of forming a sequence of pulses with a duration of 150–200 as and a repetition period of 760 as at a central wavelength of 3.37 nm in the combination of passive and active plasma of C^{5+} ions irradiated by a laser field with a wavelength of 472 nm and an intensity of $2.3 \cdot 10^{16}\,\text{W/cm}^2$ is shown. When using resonant seeding radiation with an intensity of $10^{12}\,\text{W/cm}^2$, the intensity of the generated pulses reaches $2.7 \cdot 10^{13}\,\text{W/cm}^2$ ($1.1 \cdot 10^{13}\,\text{W/cm}^2$ when the central component of the radiation spectrum is attenuated to the level of side frequencies), which is an order of magnitude greater than when the pulses are formed directly in the active medium of a C^{5+} plasma-based X-ray laser under similar conditions [24].

The obtained pulses can be used for studying the dynamics of femto- and attosecond processes in various media, including the organic ones.

The analytical calculations presented in this paper were supported by the Russian Science Foundation (project No. 19-72-00140). O. A. Kocharovskaya is grateful to the National Science Foundation for support (project No. PHY-201-2194). V. A. Antonov thanks the Theoretical Physics and Mathematics Advancement Foundation "Basis" for personal support.

REFERENCES

1. C. Bressler and M. Chergui, *Chem. Rev.*, **104**, No. 4, 1781–1812 (2004). https://doi.org/10.1021/cr0206667
2. H. Ki, K. Y. Oang, J. Kim, and H. Ihee, *Annu. Rev. Phys. Chem.*, **68**, 473–497 (2017). https://doi.org/10.1146/annurev-physchem-052516-050851
3. K. Bennett, M. Kowalewski, J. R. Rouxel, and S. Mukamel, *PNAS*, **115**, No. 26, 6538–6547 (2018). https://doi.org/10.1073/pnas.1805335115
4. M. Buzzi, M. Först, R. Mankowsky, and A. Cavalleri, *Nat. Rev. Mater.*, **3**, 299–311 (2018). https://doi.org/ 10.1038/s41578-018-0024-9
5. P. Wernet, *Phil. Trans. R. Soc.*, **377**, No. 2145, 20170464 (2019). https://doi.org/10.1098/rsta.2017.0464
6. L. Young, K. Ueda, and M. Gühr, et al., *J. Phys. B: At. Mol. Opt. Phys.*, **51**, 032003 (2018). https://doi.org/10.1088/1361-6455/aa9735
7. F. Krausz and M. Ivanov, *Rev. Mod. Phys.*, **81**, No. 1, 163–234 (2009). https://doi.org/10.1103/RevModPhys.81.163

8. M. Wu, S. Chen, S. Camp, et al., *J. Phys. B: At. Mol. Opt. Phys.*, **49**, No. 6, 062003 (2016). https://doi.org/10.1088/0953-4075/49/6/062003

9. F. Calegari, G. Sansone, S. Stagira, et al., *J. Phys. B: At. Mol. Opt. Phys.*, **49**, No. 6, 062001 (2016). https://doi.org/10.1088/0953-4075/49/6/062001

10. P. Peng, C. Marceau, and D. M. Villeneuve, *Nat. Rev. Phys.*, **1**, 144–155 (2019). https://doi.org/10.1038/s42254-018-0015-1

11. E. A. Seddon, J. A. Clarke, D. J. Dunning, et al., *Rep. Prog. Phys.*, **80**, No. 11, 115901 (2017). https://doi.org/10.1088/1361-6633/aa7cca

12. R. Schoenlein, T. Elsaesser, K. Holldack, et al., *Phil. Trans. R. Soc.*, **377**, No. 2145, 20180384 (2019). https://doi.org/10.1098/rsta.2018.0384

13. H. Daido, *Rep. Prog. Phys.*, **65**, No. 10, 1513–1576 (2002). https://doi.org/10.1088/0034-4885/65/10/204

14. Ph. Zeitoun, G. Faivre, S. Sebban, et al., *Nature*, **431**, 426–429 (2004). https://doi.org/10.1038/nature02883

15. S. Suckewer and P. Jaegle, *Laser Phys. Lett.*, **6**, No. 6, 411–436 (2009). https://doi.org/10.1002/lapl.200910023

16. A. Rockwood, Y. Wang, S. Wang, et al., *Optica*, **5**, No. 3, 257–262 (2018). https://doi.org/10.1364/OPTICA.5.000257

17. A. Depresseux, E. Oliva, J. Gautier, et al., *Nature Photon.*, **9**, 817–821 (2015). https://doi.org/10.1038/nphoton.2015.225

18. A. K. Pandey, I. Papagiannouli, F. Sanson, et al., *Opt. Express*, **28**, No. 20, 28924–28941 (2020). https://doi.org/10.1364/OE.399339

19. E. Oliva, M. Fajardo, L. Li, et al., *Nature Photon.*, **6**, 764–767 (2012). https://doi.org/10.1038/nphoton.2012.246

20. P. Zeitoun, E. Oliva, T. T. Le, et al., *Appl. Sci.*, **3**, No. 3, 581–592 (2013). https://doi.org/10.3390/app3030581

21. T. R. Akhmedzhanov, V. A. Antonov, A. Morozov, et al., *Phys. Rev.*, **96**, No. 3, 033825 (2017). https://doi.org/10.1103/PhysRevA.96.033825

22. V. A. Antonov, K. C. Han, T. R. Akhmedzhanov, et al., *Phys. Rev. Lett.*, **123**, No. 24, 243903 (2019). https://doi.org/10.1103/PhysRevLett.123.243903

23. I. R. Khairulin, V. A. Antonov, M. Yu. Ryabikin, and O. Kocharovskaya, *Phys. Rev. Res.*, **2**, No. 2, 023255 (2020). https://doi.org/10.1103/PhysRevResearch.2.023255

24. V. A. Antonov, I. R. Khairulin, and O. Kocharovskaya, *Phys. Rev.*, **102**, No. 6, 063528 (2020). https://doi.org/10.1103/PhysRevA.102.063528

25. I. R. Khairulin, V. A. Antonov, and O. A. Kocharovskaya, *Quantum Electron.*, **50**, No. 4, 375–385 (2020). https://doi.org/10.1070/QEL17290

26. V. A. Antonov, Y. V. Radeonychev, and O. Kocharovskaya, *Phys. Rev.*, **88**, No. 5, 053849 (2013). https://doi.org/10.1103/PhysRevA.88.053849

27. Y. Avitzour and S. Suckewer, *J. Opt. Soc. Am.*, **24**, No. 4, 819–828 (2007). https://doi.org/10.1364/JOSAB.24.000819

28. D. V. Korobkin, C. H. Nam, S. Suckewer, and A. Goltsov, *Phys. Rev. Lett.*, **77**, No. 26, 5206–5209 (1996). https://doi.org/10.1103/PhysRevLett.77.5206

29. Y. V. Radeonychev, M. D. Tokman, A. G. Litvak, and O. Kocharovskaya, *Phys. Rev. Lett.*, **96**, No. 9, 093602 (2006). https://doi.org/10.1103/PhysRevLett.96.093602

30. T. R. Akhmedzhanov, V. A. Antonov, and O. Kocharovskaya, *J. Phys. B: At. Mol. Opt. Phys.*, **49**, No. 20, 205602 (2016).

31. C. Bourassin-Bouchet, S. de Rossi, and F. Delmotte, in: F. Canova and L. Poleto, ed., *Optical Technologies for Extreme-Ultraviolet and Soft X-Ray Coherent Sources*, Springer Series in Optical Sciences **197**, Springer, Berlin, Heidelberg, 151–173 (2015). https://doi.org/10.1007/978-3-662-47443-3_8

32. Q. Huang, V. Medvedev, R. van de Kruijs, et al., *Appl. Phys. Rev.*, **4**, No. 1, 011104 (2017). https://doi.org/10.1063/1.4978290